Cluster Abundance Evolution and the Sunyaev-Zeldovich Effect in Various Cosmological Models

Kenji TOMITA*)

Yukawa Institute for Theoretical Physics, Kyoto University, Kyoto 606-8502, Japan

(Received June 1, 2003)

The redshift dependence of the observed cluster abundance due to the Sunyaev-Zeldovich effect (SZE) is studied in various cosmological models, including flat and open homogeneous (CDM) models and an inhomogeneous model with a large-scale local void. The Press-Schechter formalism is used to derive the abundance at epochs in the range $0 < z < 2$, and the cluster mass limit $M_{\rm lim}$ is obtained from a flux limit for SZE. It is shown that SZE is useful for constraining the cosmological model parameters, and the abundance in the inhomogeneous model may be comparable with that in the low-density homogeneous models. The significance of relative difference of abundances in the various models is discussed.

arXiv:astro-ph/0306154v4 25 Jan 2004

§1. Introduction

The abundance of clusters has been extensively studied by many people in X-ray surveys to constrain the cosmological parameters: e.g., Bahcall and Fan,[1] Viana and Liddle,[2] Eke, Cole and Frenk,[3] and Kitayama and Suto.[4–6] The cluster abundance found in the submm survey based on the Sunyaev-Zeldovich effect (SZE) has also been studied by Haiman, Mohr and Holder,[7] Holder, Haiman and Mohr,[8,9] Kitayama, Sasaki and Suto,[10] and Fan and Chiueh.[11] This SZE survey is expected to be most important in clarifying the evolution of clusters and constraining the cosmological parameters.

In this paper we study the cluster abundance obtained in the SZE survey, whose observational conditions were set to correspond to the interferometric arrays in the AMIBA project. The cluster mass limit $M_{\rm lim}$ for deriving the abundance is determined using the expression for the flux S_ν given by Kitayama and Suto,[5] which is different from that used by Fan and Chiueh.[11] This leads to a difference in the behavior of the resulting cluster abundances from that reported in their paper.

In §2, we describe the formulation for deriving the cluster abundance in the SZE survey. In §3 we present the results in various cosmological models. Here, we first consider four representative homogeneous cosmological models: LCDM with $(\Omega_0, \lambda_0) = (0.3, 0.7)$, $h = 0.7$ and $\Gamma = 0.25$, OCDM with $(0.3, 0)$, $h = 0.7$ and $\Gamma = 0.25$, SCDM with $(1.0, 0)$, $h = 0.5$ and $\Gamma = 0.5$, and τCDM with with $(1.0, 0)$, $h = 0.5$ and $\Gamma = 0.25$, where Γ is the CDM shape parameter and $H_0 = 100h$ km s^{-1} Mpc^{-1}.

At present, most cosmological observations, including SDSS,[12] high-redshift supernovae[13–16] and WMAP,[17,18] support a flat homogeneous model with nonzero

*) E-mail: tomita@yukawa.kyoto-u.ac.jp

cosmological constant. However, the presently observed values of the Hubble constant seem to be non-uniform,[19)–24)] though they include rather large uncertainties; that is, the local median value seems to be larger than that of the global median value by a factor approximately equal to 1.2. If the non-uniformity of the Hubble constant is found to be real, we may have to use inhomogeneous models to describe the cosmological observations. In the magnitude-redshift diagram of supernovae of type Ia, moreover, the point representing the recent data[26)] with $z = 1.7$ deviates from the curve predicted by the concordant model with nonzero cosmological constant. If additional supernovae with $z > 1.5$ exhibiting a similar trend are obtained, models different from the concordant model may be needed in order to account for the data. Taking this situation into consideration, we consider here an inhomogeneous model with a large-scale local void as a representative inhomogeneous model, in which there are inner and outer homogeneous regions (I and II) and a spherical boundary.[27)–30)]

The objectives motivating our study of this inhomogeneous model are discussed in previous papers.[31),32)] The first of these objectives is the introduction of the inhomogeneity of the Hubble constant, and the second is the explanation of the accelerating behavior of SNIa in the absense of a cosmological constant. The cosmological parameters in the two regions are $(\Omega_0^{\rm I}, \lambda_0^{\rm I}) = (0.3, 0)$, $\Gamma^{\rm I} = 0.25$, $H_0^{\rm I} = 70$ km s^{-1} Mpc^{-1} in the inner region (I) and $(\Omega_0^{\rm II}, \lambda_0^{\rm II}) = (1.0, 0)$, $\Gamma^{\rm II} = 0.5$, $H_0^{\rm II} = H_0^{\rm I} \times 0.82$ in the outer region (II). It is assumed that our observer is at the center for simplicity, and the spherical boundary corresponds to a redshift $z_1 = 0.067$. For the above set of parameters, the observed magnitude-redshift relation of SNIa, including the above high redshift data, was reproduced in the inhomogeneous model.[30)] The consistency of spherically symmetric inhomogeneous models with the supernova data was recently discussed and examined also by Iguchi et al.[33)] In §3 we discuss the difference among the abundances in these various models. In §4 we have concluding remarks.

§2. Number density and SZE

2.1. *The observed number of clusters*

The comoving number density of clusters of mass M with width dM is

$$n(M)dM = \Big(\frac{2}{\pi}\Big)^{1/2} \frac{\rho_0}{M} \frac{\delta_c(z)}{\sigma_0^2} \frac{d\sigma_0}{dM} \exp\Big(-\frac{\delta_c^2(z)}{2\sigma_0^2}\Big), \tag{2·1}$$

following the Press-Schechter formalism, where ρ_0 is the present mass density of the universe, $\delta_c(z)$ is the linear density threshold for collapse at redshift z, and σ_0 is the rms linear density perturbation on the scale corresponding to M. The expressions for $\delta_c(z)$ in homogeneous models are given in Kitayama and Suto's paper[5)] (cf. their Appendix A).

The differential number of clusters is expressed as

$$\frac{dN}{dzd\Omega} = \frac{dV}{dzd\Omega} \int_{M_{\rm lim}} n(M)dM, \tag{2·2}$$

where $d\Omega$ is the solid angle element, dV is the comoving volume element, and $M_{\rm lim}$ is the lower limit of the observed cluster mass, which is discussed in the next subsection. Here, the comoving volume element dV is given by

$$dV = ct\ [d_{\rm A}(z)]^2 d\Omega (1+z)^3, \tag{2·3}$$

where $d_{\rm A}$ is the angular diameter distance. Following Viana and Liddle,[2] we assume σ_0 in the form

$$\sigma_0 = \sigma_8(z)\Big(\frac{R}{8h^{-1}{\rm Mpc}}\Big)^{-\gamma(R)}, \tag{2·4}$$

where $\gamma(R) = (0.3\Gamma + 0.2)[2.92 + \log_{10}(R/8h^{-1}{\rm Mpc})]$, with $M \equiv \frac{4}{3}\pi\rho_0 R^3$, and we have

$$\sigma_8(z) = \sigma_8(0) g(\Omega(z), \lambda(z))/[(1+z)\ g(\Omega_0, \lambda_0)], \tag{2·5}$$

where $g(\Omega, \lambda)$ is an approximate factor representing the growth of linear density perturbations (Carroll, Press and Turner[34]), given by

$$g(\Omega, \lambda) = \frac{5}{2}\Omega/[\Omega^{4/7} - \lambda + (1+\Omega/2)(1+\lambda/70)], \tag{2·6}$$

and $\Omega(z)$ and $\lambda(z)$ are Ω and λ at the epoch z.

For homogeneous models the observed values of $\sigma_8(0)$ have been derived by several groups: for instance, $\sigma_8(0)\Omega_0^{0.45} = 0.53 \pm 0.05$ for $\lambda_0 = 0$ and $\sigma_8(0)\Omega_0^{0.53} = 0.53 \pm 0.05$ for $\Omega_0 + \lambda_0 = 1$ by Pen[35] and Eke et al.,[3] $\sigma_8(0)\Omega_0^{0.60} = 0.50 \pm 0.04$ by Pierpaoli et al.,[36] $\sigma_8(0)\Omega_0^{0.6} = 0.345 \pm 0.05$ by Fisher et al.,[37] $\sigma_8(0)\Omega_0^{0.5} = 0.33 \pm 0.03$ by Bahcall et al.,[38] $\sigma_8(0)\Omega_0^{0.48-0.27\Omega_0} = 0.38$ by Viana, Nichol and Liddle[39] and $\sigma_8(0)\Omega_0^{0.5} = 0.48 \pm 0.12$ by Spergel et al.[18] for the WMAP data. Here we adopt the following two sets of values:

$$\sigma_8(0)\Omega_0^p = 0.4 \text{ and } 0.5, \tag{2·7}$$

where p is 0.45 and 0.53 for models with $\lambda_0 = 0$ and flat models with $\Omega_0 + \lambda_0 = 1$, respectively.

2.2. *The lower mass limit* $M_{\rm lim}$

When photons pass through a cluster of hot electrons, a temperature decrease results and the black-body spectrum is distorted due to inverse Compton scattering as

$$\Delta T/T_{\rm CMB} = g(x) y, \tag{2·8}$$

where the Compton y-parameter is

$$y \equiv \int n_e \sigma_{\rm T} \Big(\frac{kT_{\rm gas}}{m_e c^2}\Big) dl, \tag{2·9}$$

$$g(x) \equiv \frac{x}{\tanh(x/2)} - 4. \tag{2·10}$$

Here, $x \equiv h\nu/(kT_{\rm CMB}), where \nu$ is the CMB photon frequency, n_e is the electron number density, $\sigma_{\rm T}$ is the Thomson cross section, $T_{\rm gas}$ is the temperature of the

cluster gas, and the integration is along the line of sight. If $T_{\rm gas} \gg T_{\rm CMB}$, the flux of CMB photons changes from $S_\nu^{\rm CMB}$ ($\equiv (2h\nu^3/c^2)/(e^x-1)$) to

$$S_\nu = S_\nu^{\rm CMB} \frac{xe^x}{e^x-1} g(x) Y, \tag{2·11}$$

where

$$Y = [d_{\rm A}]^{-2} \int y dA, \tag{2·12}$$

with dA the element of the projected area of a cluster. For $\nu = 219$ GHz, we have $g(x) = 0$. For $\nu < 219$ GHz, $g(x) < 0$, and for $\nu > 219$ GHz, $g(x) > 0$ In the Array for Microwave Background (AMIBA) project (Fan and Chiueh[11]), the parameters are $\nu = 90$ GHz and $x \approx 1.58$, which we use in the following. For an isothermal cluster with constant gas mass fraction, we have

$$Y = \frac{\sigma_{\rm T}}{2m_e m_p} [d_{\rm A}]^{-2} f_{\rm ICM}(1+X) k T_{\rm gas} M, \tag{2·13}$$

where m_p is the photon mass, X is the hydrogen mass fraction, and $f_{\rm ICM} \equiv \Omega_{\rm B}/\Omega_0$ for the present baryon density parameter $\Omega_{\rm B}$. For an isothermal gas, $T_{\rm gas}$ is related to the total cluster mass M by

$$kT_{\rm gas} = 5.2\gamma(1+z)\Big(\frac{\rho_{\rm vir}(z)}{18\pi^2}\Big)^{1/3}\Big(\frac{M}{10^{15}h^{-1}M_\odot}\Big)^{2/3}\Omega_0^{1/3}{\rm kev}, \tag{2·14}$$

as shown by Kitamura, Sasaki and Suto,[10] and the expression for $\rho_{\rm vir}(z)$ (which is the ratio of the mean density of the virialized cluster to the mean density of the universe at each epoch) is given in the paper of Kitamura and Suto[5] (cf. their Appendix A). Here, z is the redshift for cluster formation in principle, but it is regarded here as the redshift at the epoch in which the cluster exists. Then, the total flux of the cluster is

$$S_\nu = 25.5h(1+z)\bar{g}(x)\frac{1+X}{2} \times \frac{\Omega_{\rm B}}{\Omega_0^{2/3}}\Big[\frac{d_{\rm A}(z)}{c/H_0}\Big]^{-2}\Big(\frac{\rho_{\rm vir}(z)}{18\pi^2}\Big)^{1/3}\Big(\frac{M}{10^{15}h^{-1}M_\odot}\Big)^{5/3}\ {\rm mJy}, \tag{2·15}$$

where $\bar{g}(x)$ is given by $\bar{g}(x) \equiv x^4 e^x (e^x-1)^{-2} g(x)$. This expression is different from that given in Fan and Chiueh's paper, based on Eke, Cole and Frenk,[3] mainly with respect to Ω_0. This difference seems to result from the difference in treating the gas mass fraction as given by $\Omega_{\rm B}/\Omega_0$ or as fixed.

§3. Cluster abundance in various models

In this section we assume that the limiting flux $(S_\nu)_{\rm lim}$ is 6.2 mJy, corresponding to the AMIBA design, and calculate the limiting mass $M_{\rm lim}$ using Eq. (2·15). Then, by integrating Eq. (2·2), the differential number density of SZE clusters, $dN/(dzd\Omega)$, is obtained. In the following, we carry on this calculation for various models mentioned in §1, namely, the homogeneous models (LCDM, OCDM, SCDM and τCDM)

and an inhomogeneous model with two homogeneous regions I and II, which correspond locally to OCDM and SCDM, respectively. The four homogeneous models correspond to $(\Omega_0, \lambda_0) = (0.3, 0.7), (0.3, 0), (1.0, 0)$ and $(1.0, 0)$, respectively, and $\Gamma = 0.25$, except for SCDM with $\Gamma = 0.5$, where Γ is the CDM shape parameter.

3.1. *Homogeneous models*

In Figs. 1 and 2 the types of behavior exhibited by $dN/(dzd\Omega)$ in the four homogeneous models are shown for the two sets ($\sigma_8(0)\Omega_0^p = 0.5$ and 0.4) given in Eq. (2·7). Here, we use units of deg^{-2} and set $\Omega_{\rm B}h^2 = 1.70 \times 10^{-2}$. It is found that (1) the peaks in the low-density models are at epochs $z = 0.17$ and 0.07 for $\sigma_8(0)\Omega_0^p = 0.5$ and 0.4, respectively, and the number density decreases as a function of z more slowly for larger $\sigma_8(0)$, and (2) for $z = 0.2$, the number density in LCDM is larger by factors > 10 than that in SCDM in both cases of $\sigma_8(0)$. This trend of latter behavior is the same as that seen in Fig. 3 of the paper of Holder et al.,[8] but it is different from the behavior displayed in Fig. 1 of the paper of Fan and Chiueh.[11] This difference comes mainly from that of the factor Ω_0 used in the expressions of S_ν in the two approaches.

Next, we consider the ratio r of the number $[N(< 0.5)]$ of clusters with $z < 0.5$ to the number $[N(> 1.0)]$ of clusters with $z > 1.0$ in various models, following Fan and Chiueh. In Table I, the ratios for OCDM and LCDM are listed, while the ratio for SCDM is omitted, because it is very large compared with that for the other two models. It is found that the ratio r is sensitive to the value of $\sigma_8(0)$ as well as the model parameters. Accordingly, the observation of r may yield a significant constraint on them.

Table I. The ratio $r \equiv N(< 0.5)/N(> 1.0)$ in various models for two values of $\sigma_8(0)(\Omega_0)^p$, where p is 0.45 and 0.53 for models with $\lambda_0 = 0$ and flat models with $\Omega_0 + \lambda_0 = 1$.

$\sigma_8(0)(\Omega_0)^p$	models	ratio r
0.5	OCDM $(0.3, 0.0)$	2.67
	LCDM $(0.3, 0.7)$	25.0
	Inhom. $(\zeta^2 = 2.2)$	141
	Inhom. $(\zeta^2 = 2.0)$	269
	Inhom. $(\zeta^2 = 1.8)$	586
0.4	OCDM $(0.3, 0.0)$	19.5
	LCDM $(0.3, 0.7)$	442
	Inhom. $(\zeta^2 = 2.2)$	4.91×10^3
	Inhom. $(\zeta^2 = 2.0)$	1.33×10^4
	Inhom. $(\zeta^2 = 1.8)$	4.56×10^4

3.2. *Inhomogeneous cosmological models*

Here, we consider the inhomogeneous model with inner and outer homogeneous regions, as described in §1. For use of the Press-Schechter formalism in the two regions, we assume different spherical collapses in the two regions separately. Accordingly, when we use Eq. (2·15) for S_ν, the parameters $\Omega_0^{\rm I}$ and $\Omega_0^{\rm II}$ in the homogeneous models are used in the inner and outer regions, respectively. Because the inhomogeneity is assumed to form from an adiabatic perturbation, the ratio of

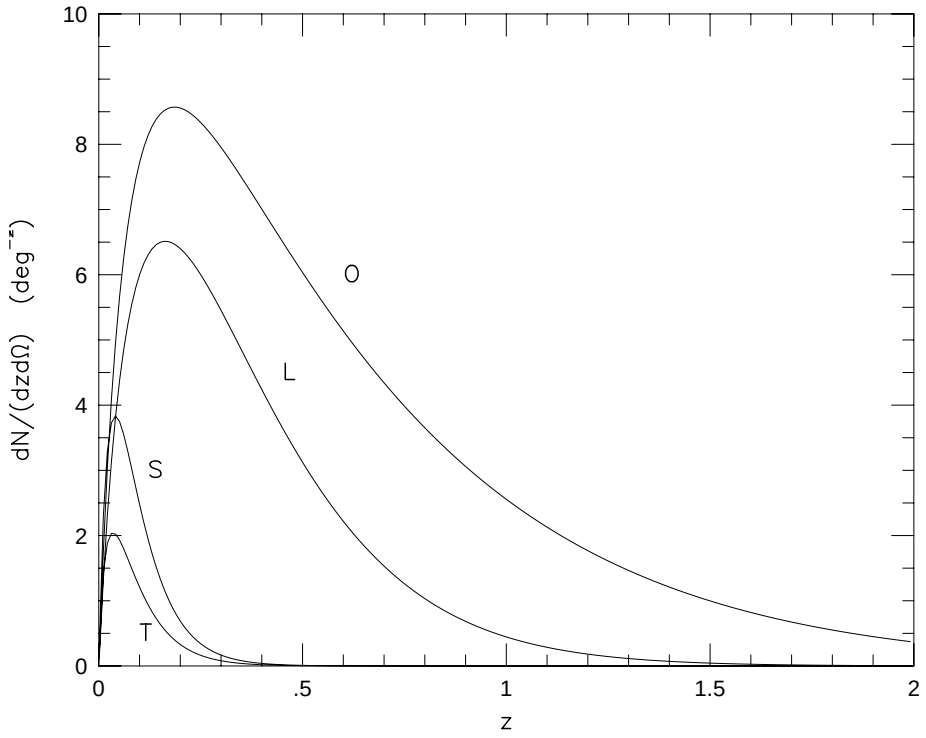

Fig. 1. $dN/(dzd\Omega)$ for $\sigma_8(0)\Omega_0^p = 0.5$ in homogeneous models. L and O denote the models (LCDM and OCDM) with $(\Omega_0, \lambda_0) = (0.3, 0.7)$ and $(0.3, 0)$, respectively, in which $\Gamma = 0.25$ and $h = 0.7$. S and T denote the Einstein-de Sitter models, in which $\Gamma = 0.5$ and 0.25, respectively, and $h = 0.5$.

the baryon density parameter to the total density parameter is equal in the two regions; that is, we have $\Omega_{\rm B}^{\rm II}/\Omega_0^{\rm II} = \Omega_{\rm B}^{\rm I}/\Omega_0^{\rm I}$. This ratio has the value 0.116 for ${\Omega_{\rm B}^{\rm I}h_{\rm I}}^2 = 0.017$. In this case, we have ${\Omega_{\rm B}^{\rm II}h_{\rm II}}^2 = 0.029$, which is consistent with the value ~ 0.025 derived from the measurement of the deuterium abundance using high-redshift QSOs,[40] while the inner value ${\Omega_{\rm B}^{\rm I}h_{\rm I}}^2 = 0.017$ is also consistent with the locally observed value.[41] Moreover, the value of $\rho_{\rm vir}^i$ corresponds to Ω_0^i

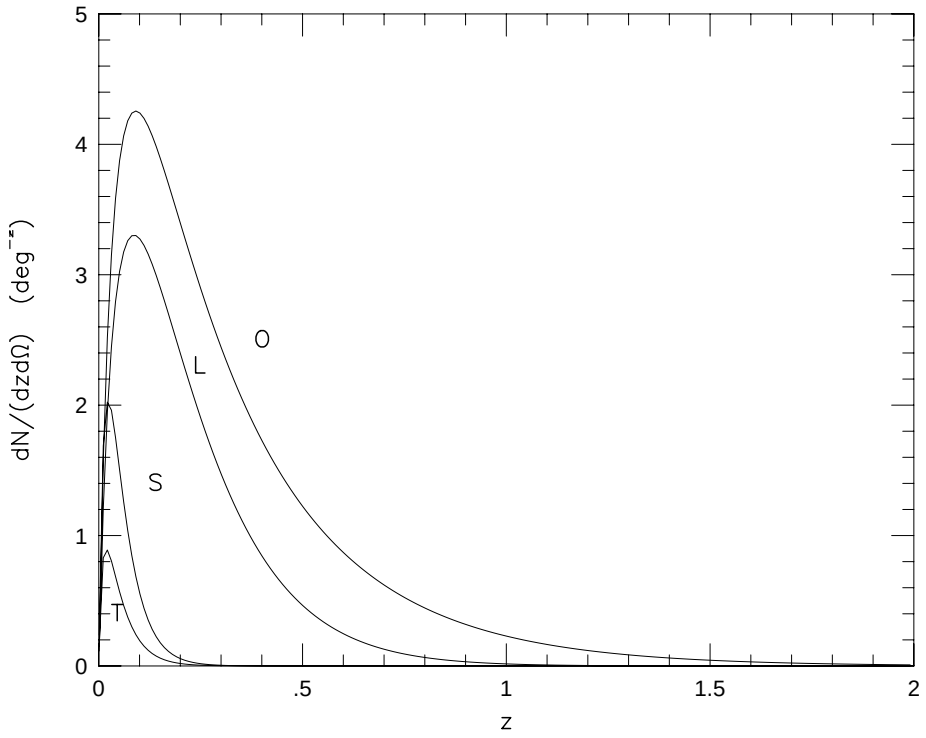

Fig. 2. $dN/(dzd\Omega)$ for $\sigma_8(0)\Omega_0^p = 0.4$ in homogeneous models. L and O denote the models (LCDM and OCDM) with $(\Omega_0, \lambda_0) = (0.3, 0.7)$ and $(0.3, 0)$, respectively, in which $\Gamma = 0.25$ and $h = 0.7$. S and T denote the Einstein-de Sitter models, in which $\Gamma = 0.5$ and 0.25, respectively, and $h = 0.5$.

for each i, and for the angular-diameter distance $d_{\rm A}$, we use the expression in the inhomogeneous model given in previous papers.[27),29)]

The inner value of σ_8, $[\sigma_8(0)]^{\rm I}$, can be determined through local observations, in the same way as in homogeneous models using

$$[\sigma_8(0)]^{\rm I}(\Omega_0^{\rm I})^p = 0.5 \text{ or } 0.4. \tag{3·1}$$

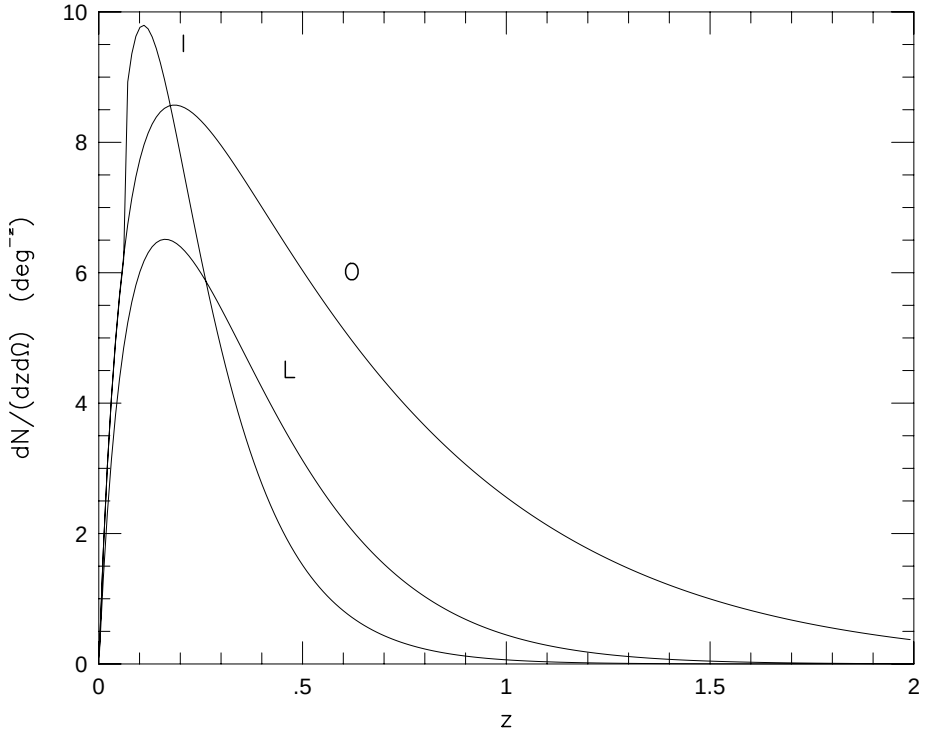

Fig. 3. $dN/(dzd\Omega)$ for $\sigma_8(0)\Omega_0^p = 0.5$ in an inhomogeneous model (I) with $\zeta^2 = 2.0$ in comparison with the two homogeneous models L and O.

In the outer region II, on the other hand, it is to be noted that $[\sigma_8(0)]^{\rm II}$ is larger than the local value ($[\sigma_8(0)]_{\rm loc}$) given in the inner region by the local observations, because the growth rate of density perturbations and the two-point correlation functions (of clusters) in the outer region are larger than those in the inner region, due to the difference between the model parameters. As a result, the present correlation function in the outer region also is larger than that in the inner region for a given same initial amplitude of density perturbations. Here, from the definitions of $\sigma_8(0)$ and the two-point correlation function $\xi(R)$ (see Suto's review paper,[42] for instance),

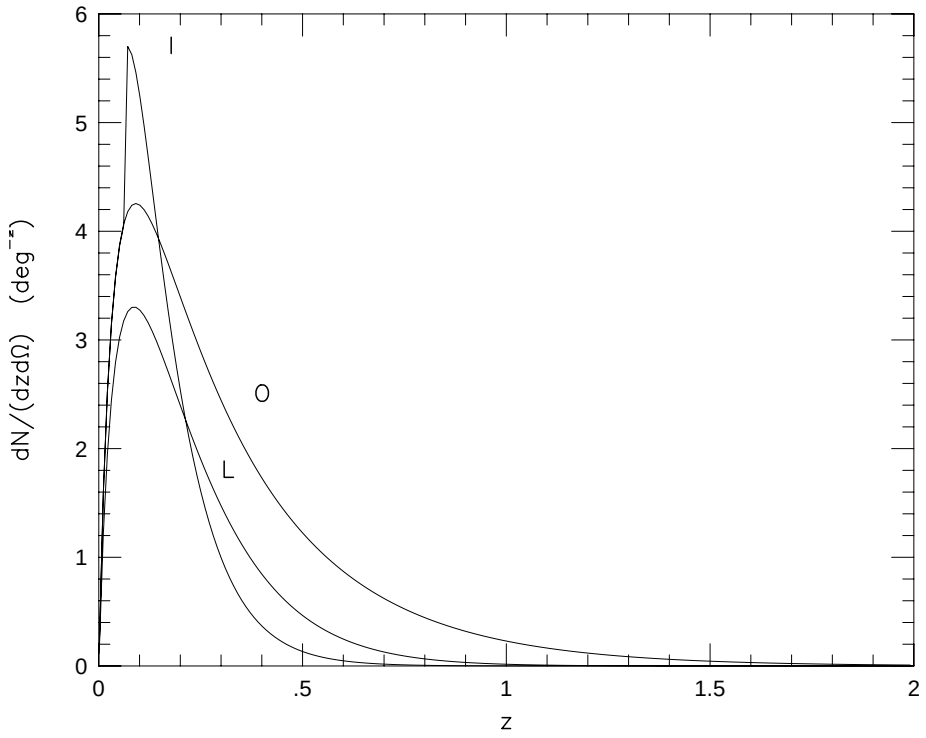

Fig. 4. $dN/(dzd\Omega)$ for $\sigma_8(0)\Omega_0^p = 0.4$ in an inhomogeneous model (I) with $\zeta^2 = 2.0$ in comparison with the two homogeneous models L and O.

$\sigma_8(0)$ and $[\xi(R)]^{1/2}$ for a fixed distance R are proportional for a given same functional form of the power spectrum. For the model parameters we use in the regions I and II, the ratio of the correlation functions ($\equiv \zeta^2$) is found to be of order 2, according to the theoretical analyses of Ref 32). For the local value of $\sigma_8(0)$ specified by

$$[\sigma_8(0)]_{\rm loc}(\Omega_0^{\rm II})^p \equiv 0.5 \text{ or } 0.4, \tag{3·2}$$

therefore, we can adopt the value of $\sigma_8(0)$ in the region II given by

$$[\sigma_8(0)]^{\rm II} = \zeta[\sigma_8(0)]_{\rm loc}, \tag{3·3}$$

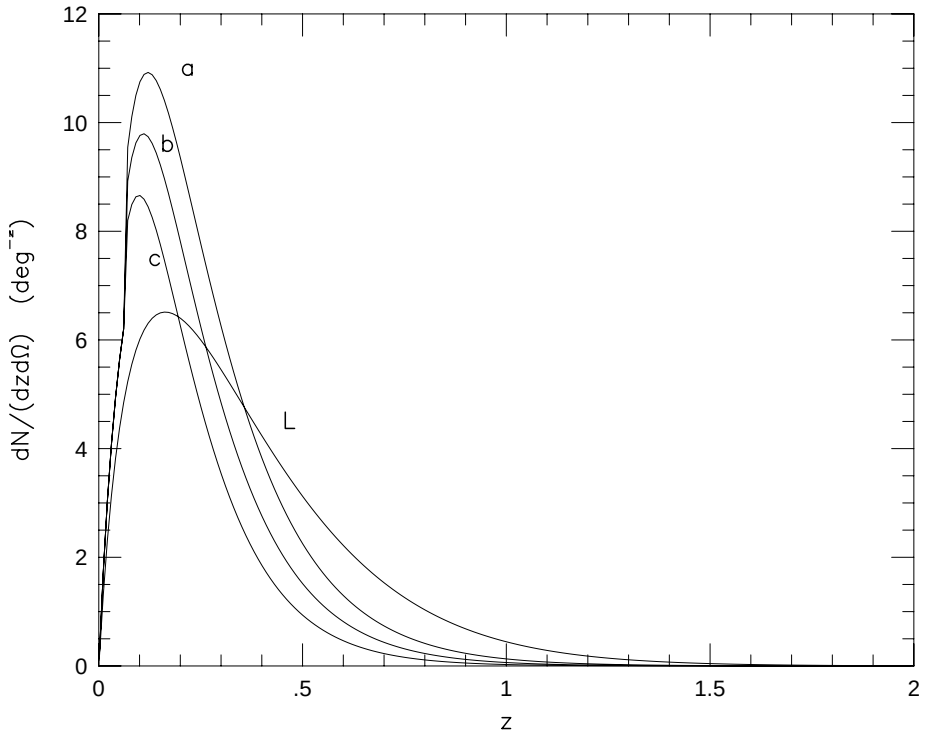

Fig. 5. $dN/(dzd\Omega)$ for $\sigma_8(0)\Omega_0^p = 0.5$ in inhomogeneous models with $\zeta^2 = 2.2, 2.0$ and 1.8, which are denoted by a, b and c, respectively.

with $\zeta^2 \sim 2$. Then we have $[\sigma_8(0)]^{\rm I}/[\sigma_8(0)]^{\rm II} \sim 0.3^{-0.45}/\sqrt{2} = 1.22$ for $\zeta^2 = 2$.

In Figs. 3 – 6, the types of behavior of $dN/(dzd\Omega)$ for inhomogeneous models are compared with those for homogeneous models. Here we use units of $\deg^{-2}$. In Figs. 3 and 4 (for $\sigma_8(0)\Omega_0^p = 0.5$ and 0.4) we compare the case $\zeta^2 = 2$ with the homogeneous models LCDM and OCDM. It is found from Figs. 1 – 4 that for all z, the number density of clusters in the inhomogeneous model is much larger than that in SCDM and that for $z < 0.25$ (0.21), it is larger than that in LCDM for $\sigma_8(0)\Omega_0^p = 0.5$ (0.4). Also, for $z = 0.6$, it is 1/2 (1/3) of that in LCDM for $\sigma_8(0)\Omega_0^p = 0.5$ (0.4). Hence,

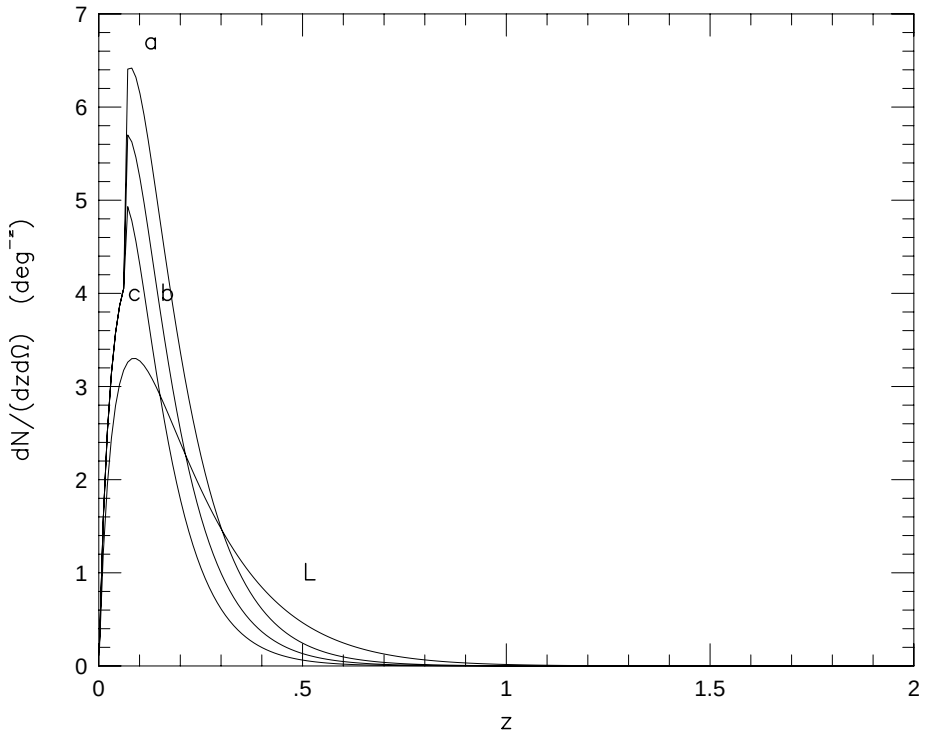

Fig. 6. $dN/(dzd\Omega)$ for $\sigma_8(0)\Omega_0^p = 0.4$ in inhomogeneous models with $\zeta^2 = 2.2, 2.0$ and 1.8, which are denoted by a, b and c, respectively.

it is concluded that SCDM can be ruled out, because of the observed existence of clusters with $z = 0.6 - 0.8$. However, the present inhomogeneous model may be consistent with the observed existence of high-redshift clusters, like LCDM.

In this inhomogeneous model, it is found on the other hand that for $z \sim 0.1$, the cluster number density in the outer region is larger by a factor of $1.5 - 2.0$ than that in the inner region, and it is large also in comparison with the number density in LCDM. In Figs. 5 and 6 (for $\sigma_8(0)\Omega_0^p = 0.5$ and 0.4) the cases with $\zeta = 2.2, 2.0$ and 1.8 are compared with the case of LCDM. It is found that the cluster number density

in the outer region depends strongly on the value of ζ, and that it decreases as a function of z more slowly for larger $\sigma_8(0)$. If ζ were equal to 1.0, the cluster number density in the outer region would reduce to that in the S model. The observation of the cluster number density for $z \sim 0.1$, therefore, may provide a stringent constraint on the value of ζ.

The physical explanation of the behavior discussed above is basically that more clusters form in the outer region because the growth rate of density fluctuations there is larger than in the inner region and is characterized by a value of ζ larger than unity.

In Table I, values of the ratio r are listed for $\sigma_8(0)\Omega_0^p = 0.5$ and 0.4 and for $\zeta^2 = 2.2, 2.0$ and 1.8. This shows that the ratio r increases with ζ and that r in the inhomogeneous model with $\zeta^2 = 2.0$ is larger by a factor ~ 10 than r in the LCDM.

§4. Concluding remarks

In the inhomogeneous model, the cluster number density in the outer region is larger than that in the inner region, as shown in the previous section. On the other hand, the galactic number densities in the two regions are nearly equal, as found in observational galactic surveys and studied theoretically in inhomogeneous models. We find that the number of galaxies within clusters in the outer region is smaller (by a factor of $1.5 - -2.0$) than that in the inner region, and therefore the mass-luminosity ratio M/L in the outer region may be larger than that in the inner region by the same factor, as long as L of clusters is produced by galaxies within clusters. This result is interesting in connection with the observation of M/L of clusters made by Bahcall and Comerford[43] (cf. their Table I), in which we find that the mean value of M/L for clusters with $z > 0.07$ is larger by a factor of ~ 1.7 than that for clusters with $z < 0.07$.

For the observed values of $\sigma_8(0)$, the values obtained from the cluster abundance in the region $z < 0.1$[3),35),36)] seem to be larger by a factor ~ 1.5 than the values in the region $z > 0.1$.[38),39)] The difference between $\sigma_8(0)$ in these two regions may be due to the uncertainties, but if it is real, it may suggest the inhomogeneity of $\sigma_8(0)$. This is also interesting from the viewpoint of our inhomogeneous models, because $\sigma_8(0)$ in the inner region is larger by a factor ~ 1.2 than $\sigma_8(0)$ in the outer region.

The above-described characteristic behavior of the cluster abundance in the outer region of our inhomogeneous models will, moreover, be similarly found not only through the Sunyaev-Zeldovich effect, but also through X-ray and usual optical observations. A comparison of the theoretical and observational results for the latter methods with $2 \geq \zeta > 1$ may give some interesting and severe constraints on the value of ζ. This must be studied subsequently.

If the observed inhomogeneity of the Hubble constant is indeed real, it cannot be explained by homogeneous models but only by inhomogeneous models, while the accelerating behavior of SN1a can be explained also by models with a Hubble constant inhomogeneity. Therefore, we finally add that more accurate measurements of the Hubble constant in gravitational lensing and SZE are desired.[44] The data for $z = 1.7$[26)] are naturally consistent with the inhomogeneous model with $(\Omega_0^{\rm I}, \Omega_0^{\rm II}) =$

$(0.3, 1.0)$,[30] while the consistency with LCDM has been argued as being due to the possible contribution of gravitational lensing to these data.[45)–47)] To clarify this difference, we must wait for the day when many data of SN1a with $z > 1.5$ are obtained.

Acknowledgements

The author thanks A. Taruya for helpful discussions on the $\sigma_8(0) - \Omega_0$ relation and the referees for kind suggestions for improving the manuscript. This work was supported by a Grant-in Aid for Scientific Research (No. 12440063) of the Japanese Ministry of Education, Culture, Sports, Science and Technology. He also acknowledges use of the YITP computer system for numerical analyses.

References

1) N. T. Bahcall and X. Fan, Astrophys. J. **504** (1998), 1.
2) P. T. P. Viana and A.R. Liddle, Mon. Not. R. Astron. Soc. **303** (1999), 535.
3) V. Eke, S. Cole and C. Frenk, Mon. Not. R. Astron. Soc. **282** (1996), 263.
4) T. Kitayama and Y. Suto, Mon. Not. R. Astron. Soc. **280** (1996), 638.
5) T. Kitayama and Y. Suto, Astrophys. J. **469** (1996), 480.
6) T. Kitayama and Y. Suto, Astrophys. J. **490** (1997), 557.
7) Z. Haiman, J.J. Mohr and G. Holder, Astrophys. J. **553** (2001), 545.
8) G. Holder, et al., Astrophys. J. **544** (2000), 629.
9) G. Holder, Z.Haiman and J.J. Mohr, Astrophys. J. **560** (2001), L111.
10) T. Kitayama, S. Sasaki and Y. Suto, Publ. Astron. Soc. Jpn. 50 **1998** (1¿).
11) Z. Fan and T. Chiueh, Astrophys. J. **550** (2001), 547.
12) I. Zehavi et al., Astrophys. J. **571** (2002), 172.
13) B. P. Schmidt, N. B. Suntzeff, M. M. Pillips, R. A. Schommer, A. Clocchiatti, R. P. Kirshner, P. Garnavich, P. Challis et al., Astrophys. J. **507** (1998), 46.
14) A. G. Riess, A. V. Filippenko, P. Challis, A. Clocchiatti, A. Diercks, P. M. Garnavich, R. L. Gilliland et al., Astron. J. **116** (1998), 1009.
15) A. G. Riess, A. V. Filippenko, W. Li and B. Schmidt, Astron. J. **118** (2000), 2668.
16) S. Perlmutter, G. Aldering, G. Goldhaber, R. A. Knop, P. Nugent, D. E. Groom, P. G. Castro, S. Deustua et al. , Astrophys. J. **517** (1999), 565.
17) C. Bennett et al., astro-ph/0302208.
18) D. Spergel et al., astro-ph/0302209.
19) C. Keeton and C. Kochanek, Astrophys. J. **487** (1997), 42.
20) F. Courbin et al., Astron. Astrophys. **324** (1997), L1.
21) C. Fassnacht, et al., Astrophys. J. **527** (1999), 498.
22) L. Williams, Astron. J. **119** (2000), 439.
23) M. Tada and T. Futamase, Prog. Theor. Phys. **104** (2001), 971.
24) C. Kochanek, Astrophys. J. **578** (2002), 25; Astrophys. J. **583** (2003), 49; astro-ph/0204043.
25) E. Reese, J. Carlstrom, M. Joy, J. Mohr, L. Grego and W. Holzapfel, Astrophys. J. **581** (2002), 53.
26) A. G. Riess et al., Astrophys. J. **560** (2001), 49.
27) K. Tomita, Astrophys. J. **529** (2000), 26.
28) K. Tomita, Astrophys. J. **529** (2000), 38.
29) K. Tomita, Mon. Not. R. Astron. Soc. **326** (2001), 287.
30) K. Tomita, Prog. Theor. Phys. **106** (2001), 929, astro-ph/0104141.
31) K. Tomita, Astrophys. J. **584** (2003), 580.
32) K. Tomita, Prog. Theor. Phys. **108** (2002), 103, astro-ph/0203125.
33) H. Iguchi, T. Nakamura and K. Nakao, Prog. Theor. Phys. **108** (2002), 809.
34) S. Carroll, W. Press and E. Turner, Ann. Rev. Astron. Astrophys. **30** (1992), 499.
35) U.-L. Pen, Astrophys. J. **498** (1998), 60.

36) E. Pierpaoli, D. Scott and M. White, Mon. Not. R. Astron. Soc. **325** (2001), 77.
37) K. Fisher et al., Mon. Not. R. Astron. Soc. **266** (1994), 50.
38) N. Bahcall et al., Astrophys. J. **585** (2003), 182.
39) P. Viana, R. Nichol and A. Liddle, Astrophys. J. **569** (2002), L75.
40) M. Pettini and D. Bowen, Astrophys. J. **560** (2001), 41.
41) S. Ryan et al., Astrophys. J. **530** (2000), L57.
42) Y. Suto, Prog. Theor. Phys. **90** (1993), 1173.
43) N. Bahcall and J. Comerford, Astrophys. J. **565** (2002), L5.
44) M. Oguri and Y. Kawano, Mon. Not. R. Astron. Soc. **338** (2003), L25.
45) G. Lewis and R. Ibata, Mon. Not. R. Astron. Soc. **324** (2001), L25.
46) E. Mörtsell, C. Gunnarsson and A. Goobar, Astrophys. J. **561** (2001), 106.
47) N. Benítez et al., Astrophys. J. **577** (2002), L1.